NASA TECHNICAL NOTE

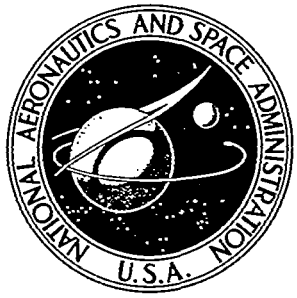

NASA TN D-6471
c.1

NASA TN D-6471

LOAN COPY: RET
AFWL (DO
KIRTLAND AFE

THERMAL DISTORTION OF A PARABOLOIDAL SHELL

by Robert J. Platt, Jr., and Marvin D. Rhodes

Langley Research Center
Hampton, Va. 23365

NATIONAL AERONAUTICS AND SPACE ADMINISTRATION • WASHINGTON, D. C. • SEPTEMBER 1971

TECH LIBRARY KAFB, NM

0133310

1. Report No.	2. Government Accession No.	3. Recipient's Catalog No.
NASA TN D-6471		

4. Title and Subtitle	5. Report Date
THERMAL DISTORTION OF A PARABOLOIDAL SHELL	September 1971
	6. Performing Organization Code

7. Author(s)	8. Performing Organization Report No.
Robert J. Platt, Jr., and Marvin D. Rhodes	L-7667
	10. Work Unit No.
9. Performing Organization Name and Address	188-78-57-01
NASA Langley Research Center Hampton, Va. 23365	11. Contract or Grant No.
	13. Type of Report and Period Covered
12. Sponsoring Agency Name and Address	Technical Note
National Aeronautics and Space Administration Washington, D.C. 20546	14. Sponsoring Agency Code

15. Supplementary Notes

16. Abstract

This paper presents the results of an experimental program to determine the deformations of a paraboloidal shell subjected to axisymmetric thermal loads. Measured local rotations of the shell surface are compared with those determined by two theoretical formulations. The results indicate generally good agreement.

17. Key Words (Suggested by Author(s))	18. Distribution Statement
Thermal distortion Paraboloidal shells	Unclassified – Unlimited

19. Security Classif. (of this report)	20. Security Classif. (of this page)	21. No. of Pages	22. Price*
Unclassified	Unclassified	24	$3.00

*For sale by the National Technical Information Service, Springfield, Virginia 22151

THERMAL DISTORTION OF A PARABOLOIDAL SHELL

By Robert J. Platt, Jr., and Marvin D. Rhodes
Langley Research Center

SUMMARY

An experimental investigation was performed at Langley Research Center to measure the distortion of a plastic paraboloidal shell subjected to axisymmetric thermal loads. The test shell was suspended in a vacuum chamber and its concave surface irradiated by a bank of tungsten lamps. Local rotations of the shell surface were determined by monitoring the motion of light rays reflected from small mirrors fixed to the convex surface of the shell.

The measured rotations of the shell surface were compared with computed rotations from two theoretical formulations. Generally, agreement between theory and experiment was good; however, some discrepancy did occur for the case of a radial-temperature increase. This discrepancy may be due, in part, to inability of the computer program to allow for radial variations of the physical properties of the shell materials.

INTRODUCTION

The prediction of distortion of paraboloidal surfaces in space due to thermal effects is of importance in the design and operation of telescopes, antennas, and solar concentrators, the last being used for power generating systems. Local surface displacements and rotations are caused by the inevitable changes in temperature that take place during operation. An analytical solution for the elastic thermal distortion of a thin paraboloidal shell is presented in reference 1. This reference includes the case of a homogeneous, isotropic shell of uniform thickness subjected to a temperature gradient (through the thickness) which is constant over the shell surface. The calculation of distortion of a shell for which the temperature varies radially as well as through the thickness may be accomplished with the generalized computer program presented in reference 2.

The present investigation was made to provide an experimental check on the validity of these analytical solutions. A 1.52-m-diameter paraboloidal shell with a depth of 0.22 m and a thickness of 0.97 cm was constructed of epoxy mixed with hollow microspheres. This shape was considered to be representative of a paraboloidal shell suitable for an antenna or a solar concentrator. The test shell was suspended in a vacuum chamber equipped with liquid-nitrogen-cooled walls (cryopanels) and irradiated on the concave

side by a bank of tungsten lamps. Local rotations of the shell surface were determined by monitoring the motion of light rays reflected from small mirrors fixed to the convex surface of the shell.

The irradiance distribution on the shell was varied to modify the shell temperature distribution and the temperature gradient through the thickness. All temperature distributions were axisymmetric. The measured change in surface angle along a meridian was compared with that calculated with the aid of references 1 and 2.

SYMBOLS

f	focal length of paraboloidal shell, meters (see fig. 5)
l	distance from mirror to light spot location, meters (see fig. 3)
R	radius of rim of paraboloidal shell, meters (see fig. 5)
R_θ	principal radius of curvature in circumferential direction, meters (see fig. 5)
R_ξ	principal radius of curvature in meridional direction, meters (see fig. 5)
r	radial coordinate, meters (see fig. 5)
ΔT	temperature difference through thickness of shell, kelvins
α	linear coefficient of thermal expansion, meters/meter-kelvin
β	meridional rotation of paraboloidal shell element, radians (see fig. 3)
δ	radial spot movement, corrected for shell radial deformation, meters (see fig. 3)
θ	circumferential coordinate, radians (see fig. 5)
ξ	meridional coordinate, meters (see fig. 5)
ϕ	angle between paraboloid axis and light beam reflected from mirror, radians (see fig. 3)

ω_θ principal curvature in circumferential direction, $1/R_\theta$, 1/meter

ω_ξ principal curvature in meridional direction, $1/R_\xi$, 1/meter

SHELL SPECIMEN AND TEST APPARATUS

Paraboloidal Shell Specimen

To validate the available theoretical solutions for the thermal distortion of a paraboloidal shell, a test model constructed of a homogeneous and isotropic material was needed. A material of low density and high stiffness was desirable to minimize distortion due to its own weight. Low thermal conductivity and a high coefficient of thermal expansion were desirable to increase the thermal distortion in order to facilitate its measurement. Epoxy plastic filled with a lightening material was selected for this application. Samples of epoxy filled with either phenolic or glass microspheres were made and tested in bending. Glass microspheres were selected as the lightening material because their use resulted in samples having nearly twice the stiffness of those made with phenolic microspheres, with little density increase. The samples made with the glass microspheres also exhibited less creep for long-term loading.

By weight, the material consisted of 67-percent epoxy resin, 9-percent catalyst, and 24-percent glass microspheres. The microspheres averaged about 100 μm in diameter. Curing temperatures were varied from 370 K to 420 K. Subsequent testing showed this variation had little effect on the bending stiffness or creep of the material. One sample was tested in tension, from which Poisson's ratio was found to be 0.3. From bending tests on three samples, Young's modulus was found to average about 2100 MN/m^2 for a density of 610 kg/m^3.

A 1.52-m-diameter glass searchlight mirror was used as a form for construction of the epoxy shell. This mirror was paraboloidal, with a maximum depth of 0.22 m and a focal length of 0.66 m. The epoxy-glass mixture was formed by hand onto the concave surface of the mirror to a thickness of about 1 cm. The open mold with epoxy-glass mixture was then placed in a chamber equipped with quartz heating lamps for curing at an elevated temperature at near atmospheric pressure. The temperature of the mixture was gradually increased to 390 K at a rate of about 8 K per hour. The lamp output was then reduced to cool the plastic at a rate of about 11 K per hour. After cooling, the paraboloidal shell was removed from the glass mold and the rather rough concave surface was sanded by hand to reduce variations in thickness. The finished paraboloidal shell averaged 0.97 cm in thickness with variations of no more than 0.056 cm except for a small region near the rim which measured 0.89 cm. The density of the material in the finished paraboloidal shell, based on these measured thicknesses and a mass of 11.5 kg, was

610 kg/m^3. At the completion of the test program, a sample was cut from the rim and its average linear coefficient of thermal expansion found to be 35×10^{-6} m/m-K for the temperature interval from 297 K to 327 K.

Thermal-Distortion Chamber and Irradiation Source

A schematic diagram of the vacuum chamber used for this test program is shown in plan view in figure 1. The chamber was 2.12 m in diameter by 2.9 m in length and was evacuated by an oil diffusion pumping system. A 1.17-m-diameter laminated glass port was located at one end of the chamber to permit transmission of the radiation from a bank of tungsten lamps to the test model. The walls, except for port openings, were covered with panels which could be cooled with liquid nitrogen. With the panels cold, the chamber pressure during testing was about 130 μN/m^2.

The test model was suspended, with the rim vertical as indicated in figures 1 and 2, by flexible strips of 0.65-cm-wide woven polyester which were cemented to the shell. The two upper supports carried the weight of the shell and the lower support was used to aline the rim of the shell in a vertical plane. Distortion of the shell due to its own weight was not apparent.

Forty-two 500-watt tungsten-filament lamps with built-in reflectors were used as a source of radiant energy to produce a thermal gradient through the test model. The lamps were arranged in four concentric groups and the output of each group was controlled by a separate variable-power transformer. The outermost ring of lamps consisted of twenty Q500R40SP-type lamps aimed at the rim of the shell. The other 22 lamps were of the 500R/3SP type and were aimed closer to the center of the paraboloid. With equal voltage applied to all lamps, the irradiance at the paraboloidal surface was measured as uniform to within ± 6 percent. The Q500R40SP lamps operated on the tungsten-halide cycle and produced a more sharply directional beam than the conventional 500R/3SP lamps. This property was needed to supply sufficient energy at the rim of the paraboloid to make the total distribution nearly uniform. The output of the lamps varied so much from lamp to lamp that it was necessary to select the lamps to be used in order to obtain acceptable uniformity.

The 1.17-m glass port consisted of three disks of 3.2-cm-thick tempered crown glass bonded with sheets of transparent plastic. The finished laminated port was about 10 cm thick. A cover glass of 1.3-cm-thick tempered crown glass was mounted parallel to the main port and separated from it by 0.13 cm. This gap formed a passage for the flow of cooling water to protect the laminated port. Measurement of the radiant energy indicated that about one-half the energy was lost in passing through the port. Most of this loss occurred in absorption by the water of nearly all lamp energy above a wavelength

of 1.4 μm. The lamps were found to produce an irradiance of the paraboloidal shell of about 0.7 solar constant, or 980 W/m^2, at the rated voltage of the lamps.

Optical Measurement System

Irradiation of the test shell by the tungsten lamps produced rotations which were measured optically at 15 points along the horizontal meridian of the shell. The optical measurement system used is shown in figures 1 and 3. Two 25-watt zirconium arc lamps served as point light sources. Each of 15 small lens-mirrors, mounted on the convex surface of the paraboloid as indicated in figure 4, returned an image of an arc lamp to one of the two viewing screens. In operation, a series of small bright spots of light was visible on each of the screens, each spot being an image of a source. Movements of the spots from their positions with the paraboloid at uniform temperature (tungsten lamps off) to their positions with a temperature gradient (lamps on) were a measure of angular changes of the surface.

Each lens-mirror was made of a 6-mm-square plane mirror to which was cemented a 6-mm-square lens with a focal length to image the point source at the screen. Each lens-mirror was cemented with epoxy to the paraboloidal surface. Where necessary, a metal wedge was cemented between the mirror and the paraboloid to obtain the needed mirror angle.

Temperature Instrumentation

The shell surface temperatures were measured by thermocouples which were cemented to the surfaces at the locations indicated in figure 4. The thermocouples were made of 0.25-mm-diameter copper-constantan wire. In order to reduce temperature measurement errors and possible influence of the leads on the shell temperatures, the leads were cemented to the surfaces and the complete test model was painted flat black. Temperatures were recorded with a multiple-point self-balancing potentiometer.

EXPERIMENTAL PROCEDURE

Each thermal-distortion test extended over 3 days. On the first day, the paraboloidal shell was suspended in the chamber and positioned so that the spots of light formed by the focusing mirrors fell on the viewing ports. The chamber was evacuated and pumping continued until the second day to provide time for the shell to stabilize in the vacuum environment. On the second day of the test, the centers of the reflected spots of light were marked on the viewing screens for a "zero" reading. Liquid nitrogen was then introduced into the cryopanels and the heating lamps turned on. In about 2 hours the temperatures reached equilibrium and the new locations of the reflected spots were marked

on the viewing screen and the temperatures recorded. In most test runs the lamp output was then changed to modify the temperatures of the shell to provide additional test points. After recording the data, the liquid-nitrogen flow was shut off and the chamber and shell slowly returned to room temperature. On the third day, with the chamber still evacuated, the spot locations were again marked on the viewing screens as a final "zero" reading.

The positions of the light spots corresponding to the initial and final zero readings differed by no more than 0.1 cm, equivalent to a rotation of about 0.5 mrad. These changes were all in the same direction, indicating a slight repositioning of the entire shell. An average of the two zero positions was used for the reduction of the data. With the heating lamps on and the cryopanels cold, the maximum deflection of the spots was about 3 cm, corresponding to a shell rotation of about 13 mrad.

The observed spot deflections on the screens were corrected for radial deformation of the shell caused by the thermal loading. The measured temperatures were used to compute the radial deformation by the program of reference 2. The maximum correction to the spot deflections for radial deformation was about 0.2 cm.

The equation used to compute the local rotations of the shell from the corrected light spot deflections was

$$\beta = \frac{\delta \cos \phi}{2l}$$

This equation was based on the viewing screen being normal to the axis of the shell and assumed that changes in ϕ and l produced by the rotations were small and could be neglected. When the computed rotations were plotted against radial location, the plotted points for some test runs seemed to indicate a discontinuity in rotation at the axis of the paraboloid. However, this could be explained by a slight rotation of the suspended paraboloid about a vertical axis while being heated. A correction for this apparent swing of the shell was made to eliminate the discontinuity and bring the value of β to zero at the axis of the paraboloid. In the worst case, this amounted to subtracting 0.6 mrad from each of the rotations measured on one side of the paraboloid and adding 0.6 mrad on the opposite side.

ANALYTICAL SOLUTIONS

The experimental data obtained in this investigation were compared with analytical results utilizing material from references 1 and 2. The analysis presented in reference 1 describes the deformation of a thin paraboloidal shell subjected to axisymmetric thermal loading. In reference 1 the equations are solved only for the cases of a uniform temperature change of the shell and a temperature gradient (through the thickness) which is constant over the shell surface. Several boundary conditions at the periphery of the shell,

including the case of an attached stiffening ring, were considered in reference 1. However, the only case of interest for comparison with the experimental data of this investigation was the special case of a free boundary.

The analysis presented in reference 2 is more general than that presented in reference 1. Reference 2 presents a generalized computer program for the finite-difference solutions of shells of revolution. In order to adapt this program for the analysis of thin paraboloidal shells, subroutines were written which mathematically describe the shell geometry and the thermal loading. The parameters necessary to describe the shell geometry are ξ, ω_θ, ω_ξ, $\frac{d\omega_\xi}{d\xi}$, and $\frac{1}{r}\frac{dr}{d\xi}$. Equations defining these parameters were derived and are shown in figure 5. The program presented in reference 2 requires that the middle surface be defined by $r = r(\xi)$. The equation relating r and ξ, shown in figure 5, cannot be readily written as $r(\xi)$. Therefore, it was necessary to program $r(\xi)$ using a fourth-order Runge-Kutta approximation. The subroutine defining $r(\xi)$ and the other parameters describing the shell geometry are shown in appendix A.

The program of reference 2 is an automated version of a finite-difference method presented in reference 3. During this investigation it was noted that several equations presented in reference 3 had not been properly programed in the "FORCE" subroutine of reference 2. These equations were reprograming and are included in the revised "FORCE" subroutine listed in appendix B. The reprograming of these equations did not significantly affect the results for the temperature distributions considered in this investigation. However, they may have a significant influence on other shell problems involving thermal gradients.

The temperatures used in the calculations were those measured by the thermocouples during the experimental investigation. A linear temperature gradient was assumed to exist through the paraboloidal shell thickness and was calculated using the measured front and back surface temperatures. All temperature variations were considered to be axisymmetric. Therefore, the temperatures measured at equal radial locations were averaged in order to obtain an axisymmetric distribution. The temperatures measured at equal radial locations were within 1 percent of the average temperature.

RESULTS AND DISCUSSION

First to be investigated were the shell rotations produced by a radially uniform temperature gradient through the shell thickness. To achieve this type of temperature gradient, cryopanels 3, 4, and 5 (see fig. 1) were filled with liquid nitrogen and all 42 lamps were turned on. The resulting temperature distributions along the horizontal meridian of the paraboloid are shown in figure 6 for two lamp voltage settings. The distribution of temperature was slightly nonuniform, with the temperature increasing near the rim on

one side and decreasing near the rim on the other. The temperature difference through the thickness was nearly constant with radial location.

The rotations of the paraboloidal shell, as measured for the temperature distributions of figure 6, are plotted in figure 7 as a function of radius. The rotation β of each mirror mounted on the shell surface has been converted to a nondimensional parameter $\frac{\beta}{\alpha\ \Delta T}$, as used in reference 1. The value used for the coefficient of thermal expansion α was measured as 35×10^{-6} m/m-K from tests on a piece cut from the shell after the vacuum-chamber tests were completed. The values of ΔT were average values obtained from the data of figure 6. These values were 25 K and 31.5 K for the two different lamp heating conditions. The experimental data for the two different lamp voltages are in good agreement and a single curve was faired through them in figure 7. The data points from one side of the paraboloidal shell are represented by unflagged symbols and from the opposite side by flagged symbols.

Shown in figure 7 for comparison with the measured values of rotation is the theoretical curve for a paraboloidal shell similar in curvature to the test shell and having a uniform thickness equal to the average thickness of the test shell. The theoretical curve shown was obtained by use of the program of reference 2. Calculations using the solution of reference 1 yielded an almost identical theoretical curve with about 1 percent less rotation at the rim. Agreement of the experimental data with the theoretical curve is considered good. As the theory predicts, the major rotation occurred at the rim, but the value measured was somewhat less than that predicted.

The investigation was extended to the case of nonuniform but axisymmetrical temperature distributions by switching off some of the lamps used to heat the paraboloidal shell. The temperature distributions resulting from this nonuniform heating are shown in figure 8. Using only the 20 outer lamps, directed at the rim of the shell, the temperatures were highest at the rim. Using only the 22 inner lamps, directed toward the central area of the shell, the temperatures were highest at the center. Ideally, the midsurface temperature would have been constant with radius and only the temperature difference through the thickness varied axisymmetrically, but this was not possible with the heating system used. The resulting radial temperature changes shown in figure 8 probably introduced some radial variation of the coefficient of thermal expansion and Young's modulus of the shell material which could not be incorporated in the analytical solution.

The measured temperatures of figure 8 were averaged to obtain a midsurface temperature and a temperature difference through the thickness, both of which varied with radius. These average temperature distributions were used, with the program of reference 2, to compute the corresponding theoretical rotations of the paraboloidal shell subjected to axisymmetric temperature distributions. The measured rotations as a function of radial station are compared in figure 9 with the theoretical rotations. In the case of

heating by the outer lamps only, the measured rotations were less than those predicted by the theory but the shapes of the curves are similar. In the case of heating by the inner lamps only, agreement was very good.

Up to this point, all the tests had been made with only cryopanels 3, 4, and 5 cold. More extreme variations of temperature with radial location were obtained by cooling all five cryopanels with liquid nitrogen. This eliminated much of the nearly uniform irradiation of the concave surface furnished by the warm walls. The lamps then supplied nearly all the radiation reaching the shell. The measured surface temperature distributions, after equilibrium was reached, are shown in figure 10. Included is the case with all the lamps turned on, which resulted in a nearly uniform temperature gradient through the thickness of the shell. For each of these three temperature conditions, the temperature distributions were averaged and the theoretical distortions computed, as before, by the program of reference 2. The theoretical rotations are compared in figure 11 with the measured rotations. Agreement is good for the uniform temperature case (all lamps on) and the radially decreasing temperature case (inner lamps only). Agreement is not as good for the radially increasing temperature case. The reason for this discrepancy is not certain, but it may be due, in part, to variations of the physical properties of the plastic with radial location which cannot be handled by the program of reference 2.

CONCLUDING REMARKS

An experimental investigation was performed at Langley Research Center to measure the distortion of a plastic paraboloidal shell subjected to axisymmetric thermal loads and the test data were compared with theoretical calculations. Local rotations of the shell surface were determined by monitoring the motion of light rays reflected from small mirrors fixed to the convex surface of the shell. For the case of a radially uniform temperature difference through the thickness of the shell, the measured rotations agreed well with two theoretical formulations. For the case of axisymmetrical temperature distributions, which combined a radially varying midsurface temperature with a radially varying temperature gradient through the shell thickness, agreement with theory was good for radially decreasing temperatures but not as good for radially increasing temperatures. Some of this discrepancy may be due to inability of the computer program to allow for radially varying physical properties of the shell material. Within this limitation, the available theory appears satisfactory for the prediction of thermal distortion of paraboloidal shells.

Langley Research Center,
National Aeronautics and Space Administration,
Hampton, Va., August 5, 1971.

APPENDIX A

SHELL-GEOMETRY SUBROUTINES

The subroutine "INPUT" necessary to calculate the shell geometry for the computer program of reference 2 is listed below. The equations represented by this listing are shown in figure 5.

```
      SUBROUTINE INPUT(NMAX)
      COMMON R(502)/BL1/GAM(502),OMT(502),OMX1(502),DEOMX(502)/BL3/NU,
     1LAM,N,EALSIG,CHAR,DEL
      READ(5,1)S,F,R(1)
    1 FORMAT(3F10.5)
      DEL=S/(CHAR*FLOAT(NMAX-2))
      K=1
      A=CHAR
      NTLAS=NMAX-1
      IF(R(1).EQ.0.0000) 2,3
    2 GAM(1)=1.E321
      GO TO 4
    3 GAM(1)=1./(R(K)*SQRT(R(K)**2*A**2/(4.*F**2)+1.))
    4 OMT(1)=1./SQRT(4.*F**2/A**2+R(K)**2)
      OMX1(1)=4.*A*F**2/(4.*F**2+A**2*R(K)**2)**1.5
      DEOMX(1)=-24.*A**3*R(K)*F**3/(4.*F**2+A**2*R(K)**2)**3
      CALL SURFAC(2,F,0.5*DEL)
      DO 5 K=3,NTLAS
      CALL SURFAC(K,F,DEL)
    5 CONTINUE
      CALL SURFAC(NMAX,F,0.5*DEL)
      DO 6 K=2,NMAX
      GAM(K)=1./(R(K)*SQRT(R(K)**2*A**2/(4.*F**2)+1.))
      OMT(K)=1./SQRT(4.*F**2/A**2+R(K)**2)
      OMX1(K)=4.*A*F**2/(4.*F**2+A**2*R(K)**2)**1.5
    6 DEOMX(K)=-24.*A**3*R(K)*F**3/(4.*F**2+A**2*R(K)**2)**3
      RETURN
      END
```

The subroutine "SURFACE" called by the subroutine "INPUT" is listed below with the necessary function subprogram.

```
SUBROUTINE SURFAC(K,F,DELTA)
COMMON R(502)/BL3/NU,LAM,N,EALSIG,CHAR,DEL
REAL K1,K2,K3,K4
K1=DELTA*VALUE(R(K-1),F,CHAR)
K2=DELTA*VALUE(R(K-1)+0.5*K1,F,CHAR)
K3=DELTA*VALUE(R(K-1)+0.5*K2,F,CHAR)
K4=DELTA*VALUE(R(K-1)+K3,F,CHAR)
R(K)=R(K-1)+(1./6.)*(K1+2.*K2+2.*K3+K4)
RETURN
END
```

APPENDIX A – Concluded

```
FUNCTION VALUE(P,F,CHAR)
C=2.*F
D=SQRT(P*P*CHAR*CHAR+4.*F*F)
VALUE=C/D
RETURN
END
```

APPENDIX B

SUBROUTINE FORCE

The corrected subroutine "FORCE" for the computer program of reference 2 is listed below.

```
      SUBROUTINE FORCE(K,INDS,NMAX)
C SUBROUTINE FORCE  THIS SUBROUTINE CALCULATES THE ELEMENTS OF THE LOWER CASE
C E-VECTOR AS DEFINED IN APPENDIX A OF REFERENCE(1),AT THE STATION SPECIFIED
C BY THE INDEX K.
      COMMON R(502)/BL1/GAM(502),OMT(502),OMX1(502),DEOMX(502)/BL3/NU,
     1LAM,N,EALSIG,CHAR,DEL/BL4/CEE(4)
      REAL NU,LAM,N,L2
      REAL MSTP
      RA=R(K)
      GA=GAM(K)
      OX=OMX1(K)
      OT=OMT(K)
      T=TEMP(K,DEL)
      DT=DTEMP(K,DEL)
      DELT1=DELT(K,DEL)
      DLT1=DDELT(K,DEL)
      PX1=PX(K,DEL)
      PT1=PT(K,DEL)
      P1=P(K,DEL)
      H=HHT(K,DEL)
      DH=DHHT(K,DEL)
      HRB=HRA(K,DEL)
      DHRB=DHRA(K,DEL)
      D1=1.-NU
      L2=LAM**2
      EAL=EALSIG
      TSUBT=2.*H*EAL/(D1*HRB)*T
      MSTP=CHAR*EAL/(3.*D1)*((1.5/HRB-3./HRB**2+2./HRB**3)*(DLT1*H**3+3.
     1*H**2*DH*DELT1)+DELT1*H**3*DHRB/HRB**2*(-1.5+6./HRB-6./HRB**2))
      CEE(4)=CHAR*EAL*DELT1*H**3/(3.*D1)*(1.5/HRB-3./HRB**2+2./HRB**3)
      CEE(1)=-PX1+2.*EAL/(D1*HRB)*(H*DT+T*DH)-DHRB/HRB*TSUBT-
     1L2*D1*GA*OX*CEE(4)
      CEE(2)=-PT1-N/RA*TSUBT-L2*D1*N/RA*D1*CEE(4)
      CEE(3)=-P1-(OX+OT)*TSUBT-L2*D1*GA*MSTP+
     1L2*D1*CEE(4)*(OX*OT-(N/RA)**2)
      RETURN
      END
```

REFERENCES

1. Walz, Joseph E.: Thermal Distortions of Thin-Walled Paraboloidal Shells. NASA TN D-3543, 1966.

2. Schaeffer, Harry G.: Computer Program for Finite-Difference Solutions of Shells of Revolution Under Asymmetric Loads. NASA TN D-3926, 1967.

3. Budiansky, Bernard; and Radkowski, Peter P.: Numerical Analysis of Unsymmetrical Bending of Shells of Revolution. AIAA J., vol. 1, no. 8, Aug. 1963.

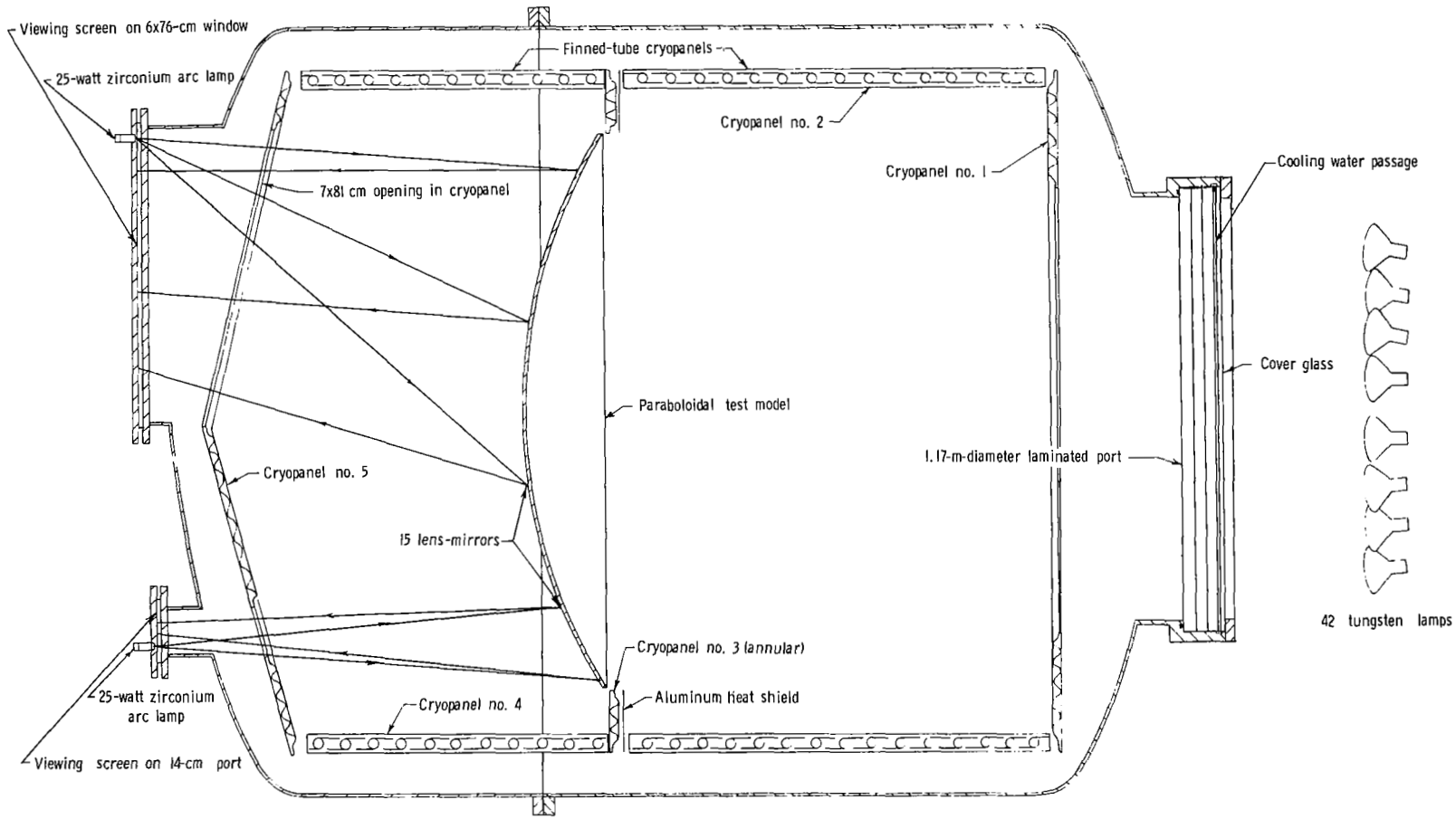

Figure 1.- Schematic diagram of thermal-distortion vacuum chamber and test apparatus.

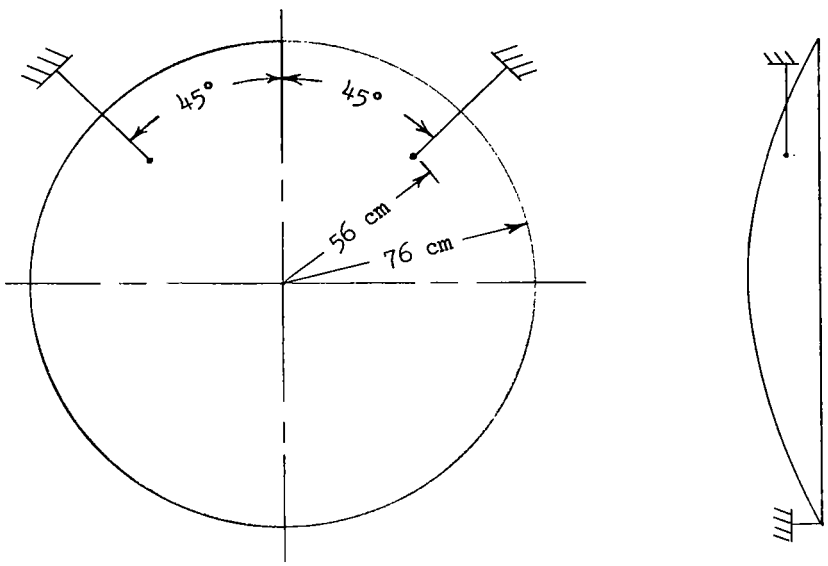

Figure 2.- Schematic drawing of the suspension system of the paraboloidal test model.

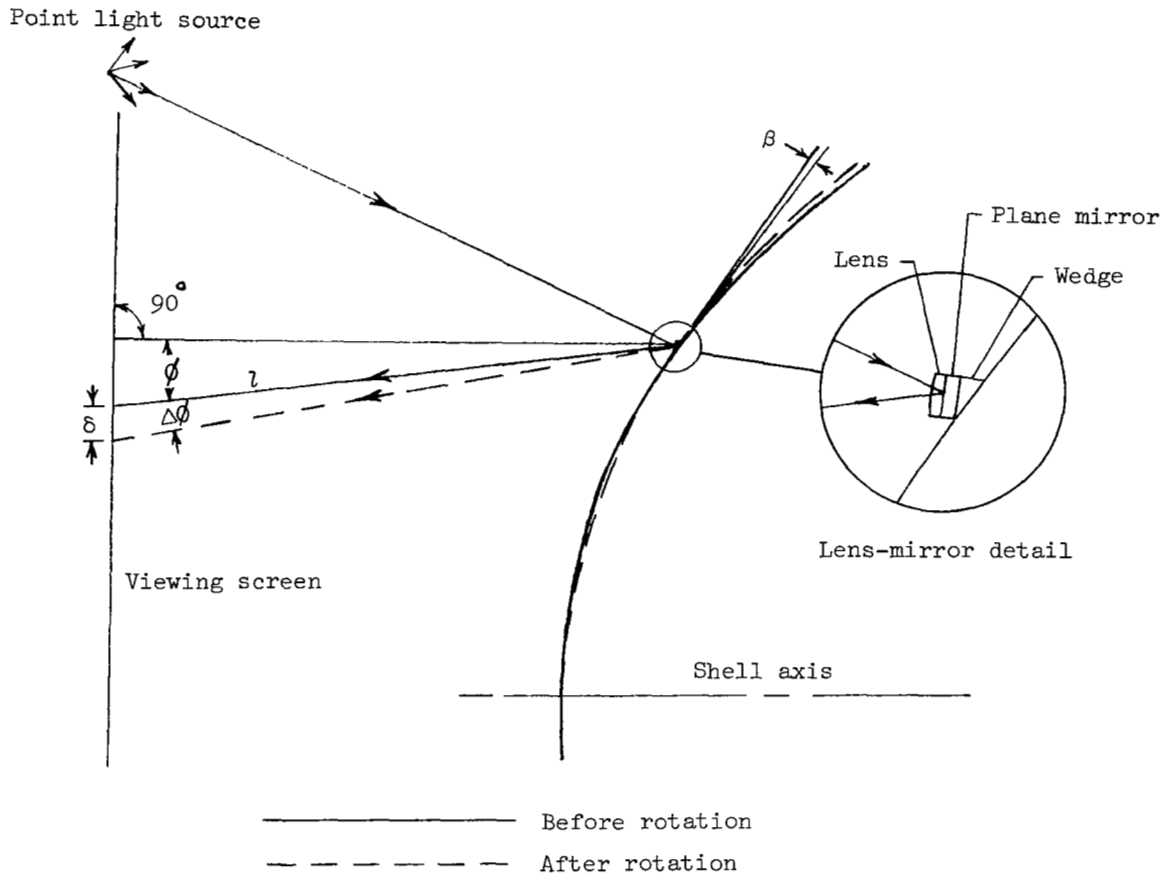

Figure 3.- Optical system for measurement of shell rotation.

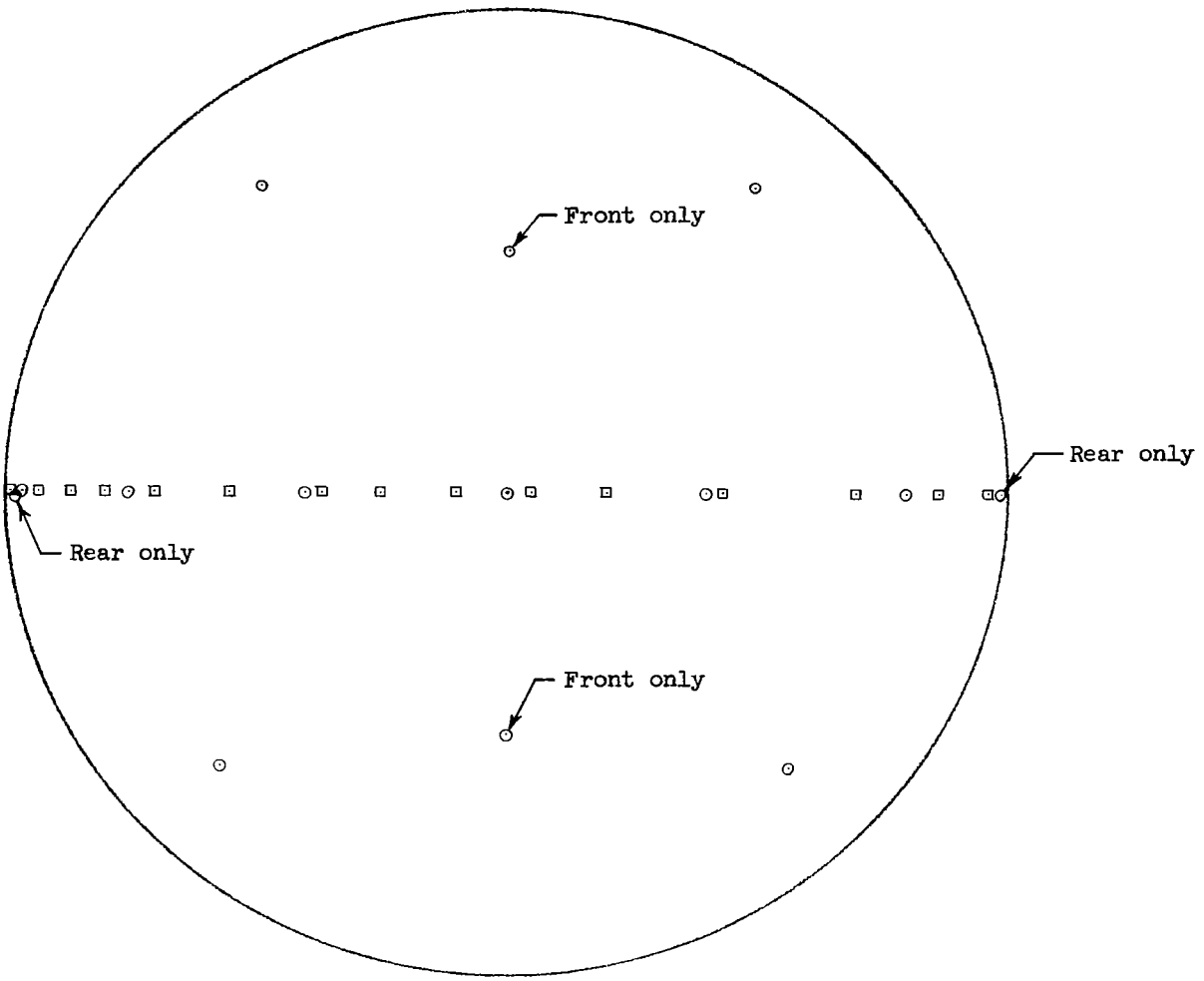

○ Thermocouple location. Unless otherwise noted, thermocouples were located on both front and rear surfaces

□ Lens–mirror location (all on rear surface)

Figure 4.- Location of thermocouples and lens-mirrors on 1.52-m-diameter paraboloidal shell.

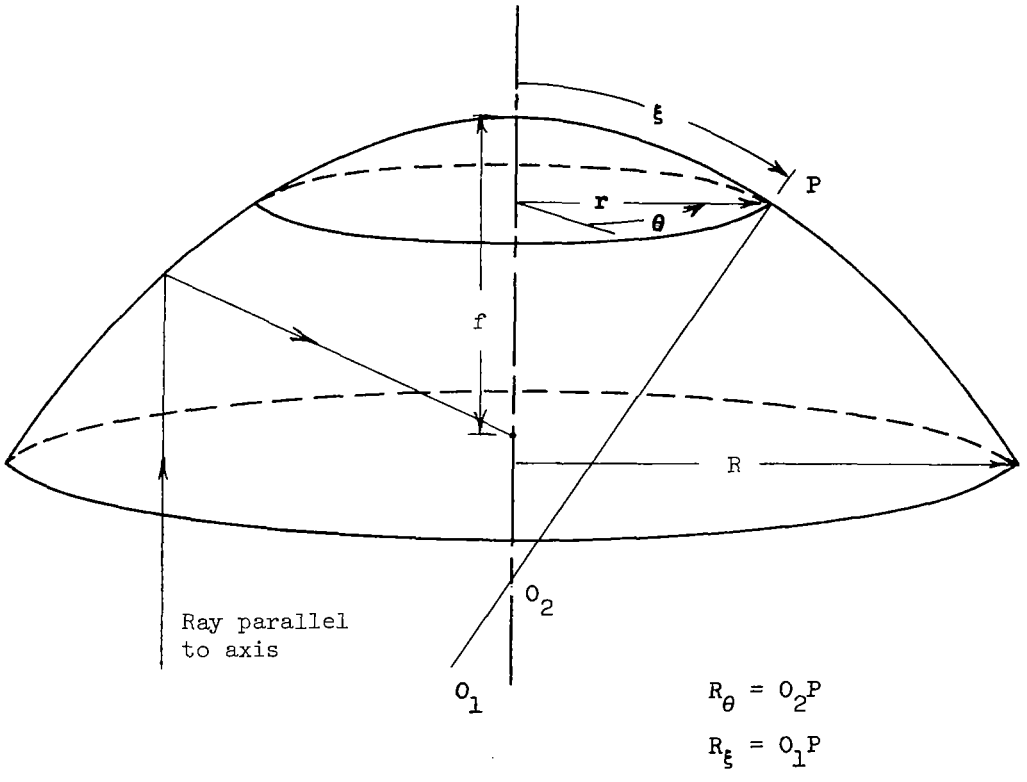

Equations defining shell geometry:

$$\xi = \frac{r}{2}\left(\frac{r^2}{4f^2} + 1\right)^{1/2} + f \ln\left[\frac{r}{2f} + \left(\frac{r^2}{4f^2} + 1\right)^{1/2}\right]$$

$$\omega_\theta = \frac{1}{R_\theta} = \left(4f^2 + r^2\right)^{-1/2}$$

$$\omega_\xi = \frac{1}{R_\xi} = 4f^2\left(4f^2 + r^2\right)^{-3/2}$$

$$\frac{d\omega_\xi}{d\xi} = -24rf^3\left(4f^2 + r^2\right)^{-3}$$

$$\frac{1}{r}\frac{dr}{d\xi} = \frac{2f}{r}\left(r^2 + 4f^2\right)^{-1/2}$$

Figure 5.- Surface geometry and coordinate system of paraboloidal shell.

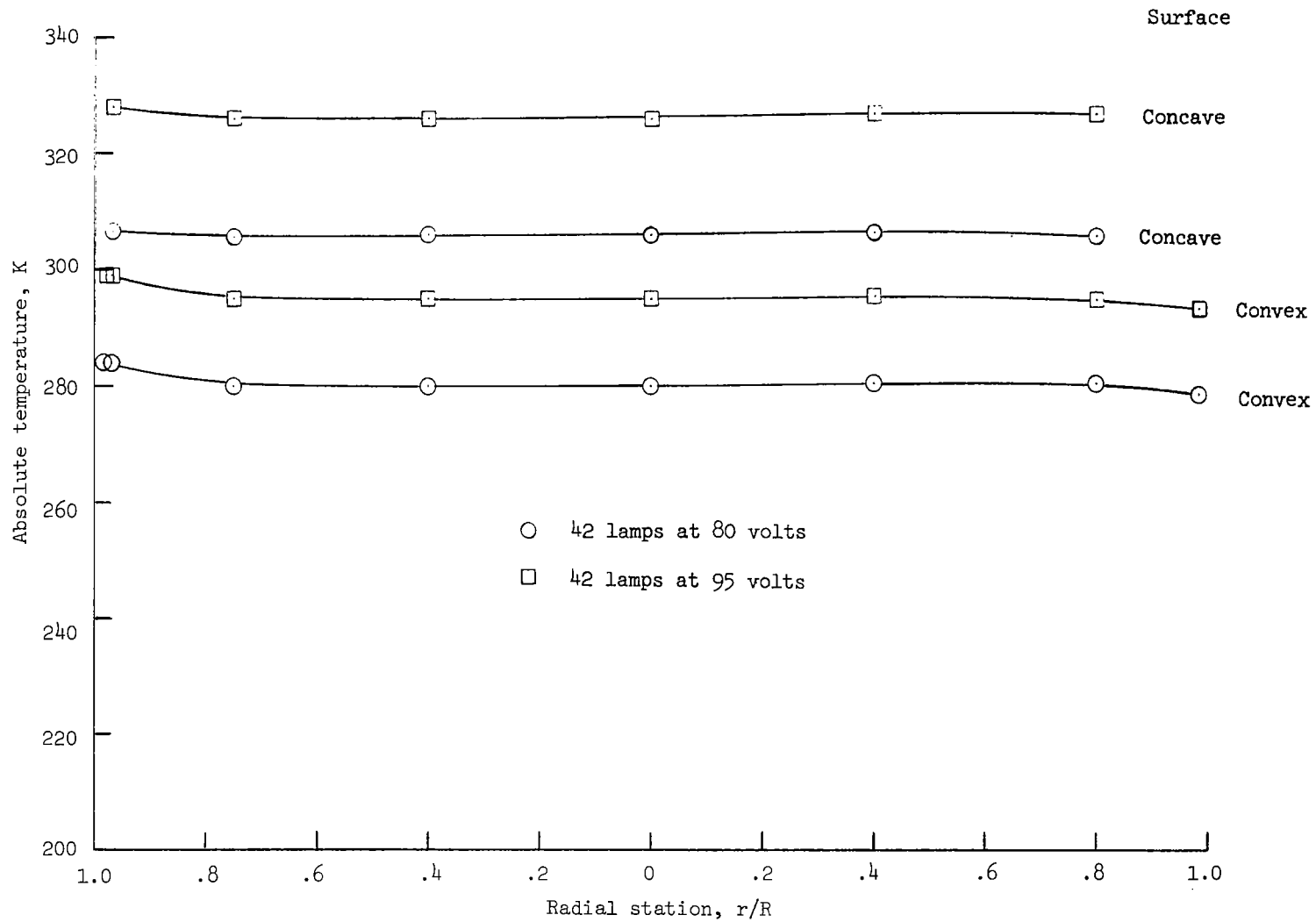

Figure 6.- Measured paraboloidal-shell surface temperatures along horizontal meridian. Cryopanels 3, 4, and 5 cold.

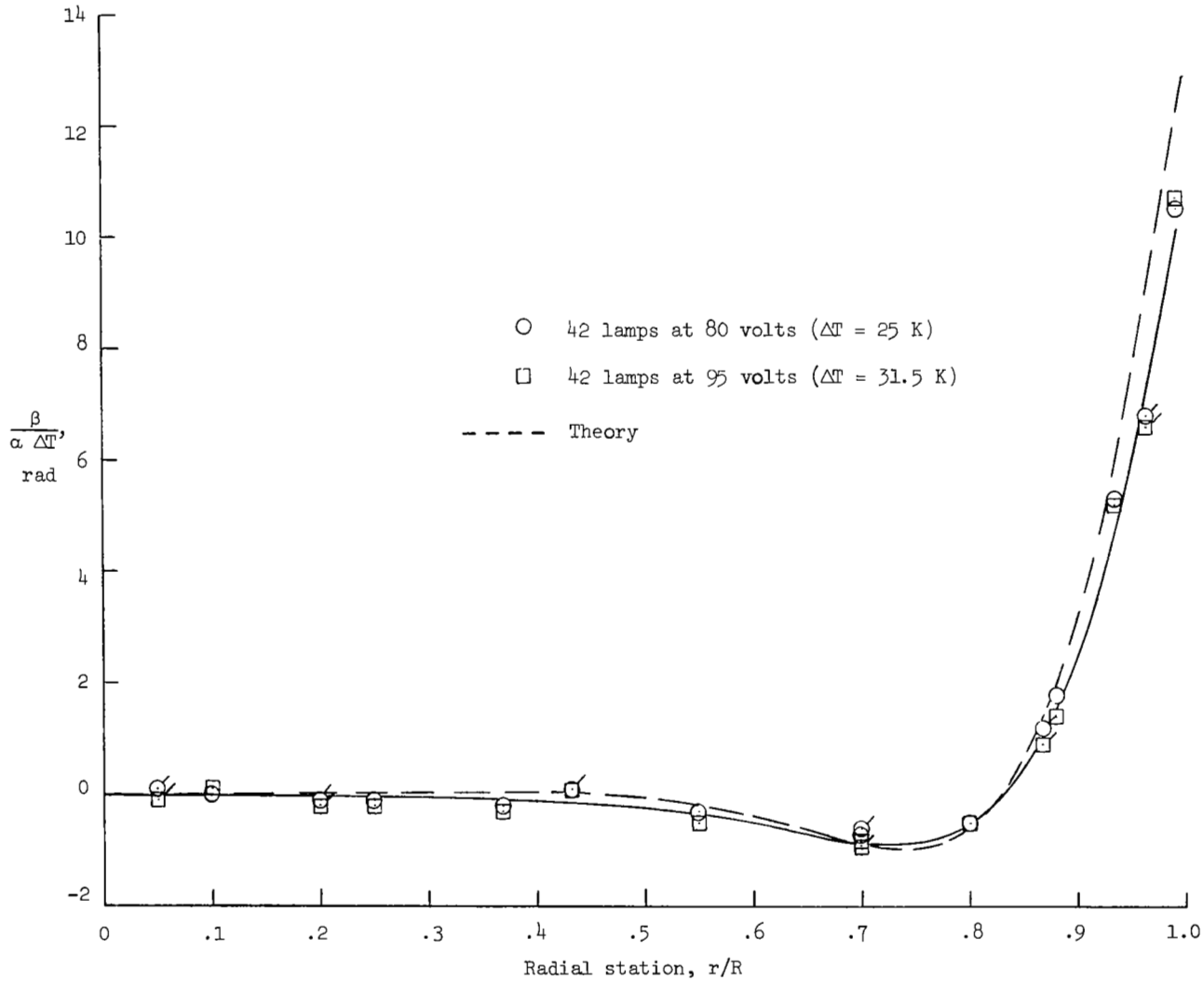

Figure 7.- Measured and theoretical rotation of paraboloidal-shell surface due to uniform temperature change through shell thickness. Flagged symbols represent right side of paraboloidal shell.

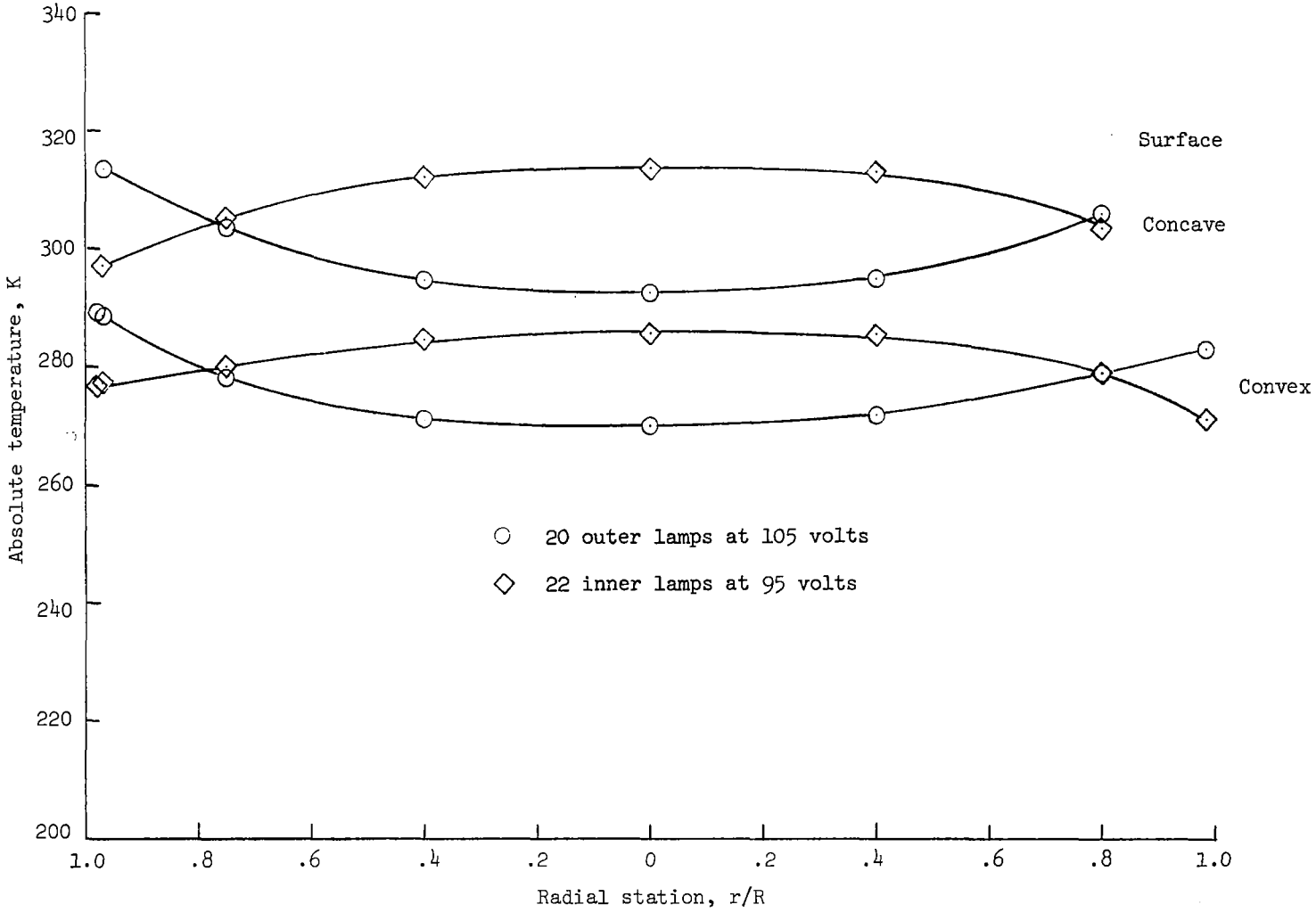

Figure 8.- Measured paraboloidal-shell surface temperatures along horizontal meridian for axisymmetrical irradiation. Cryopanels 3, 4, and 5 cold.

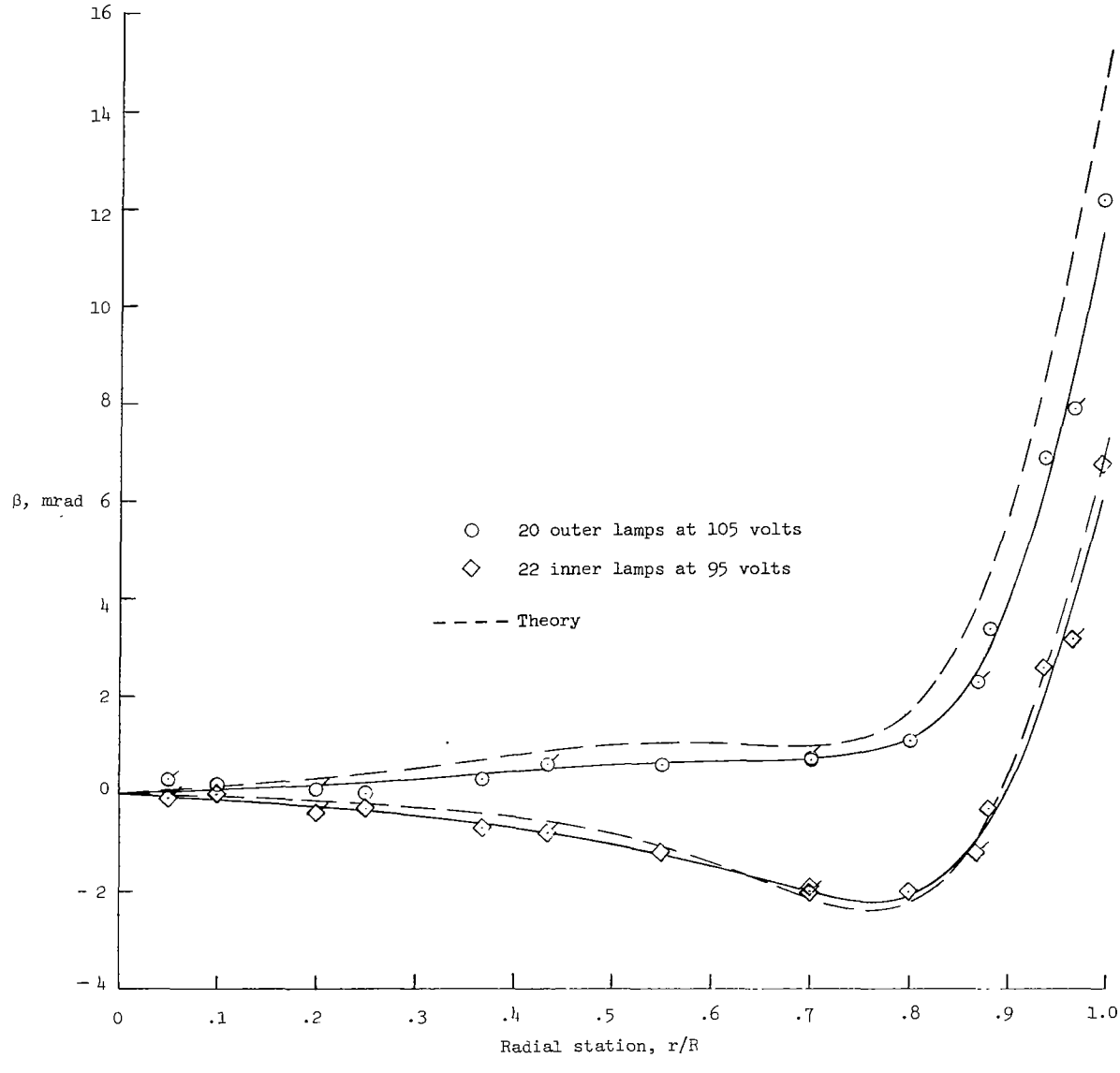

Figure 9.- Measured and theoretical rotation of paraboloidal-shell surface due to axisymmetrical temperature distributions. Cryopanels 3, 4, and 5 cold. Flagged symbols represent right side of paraboloidal shell.

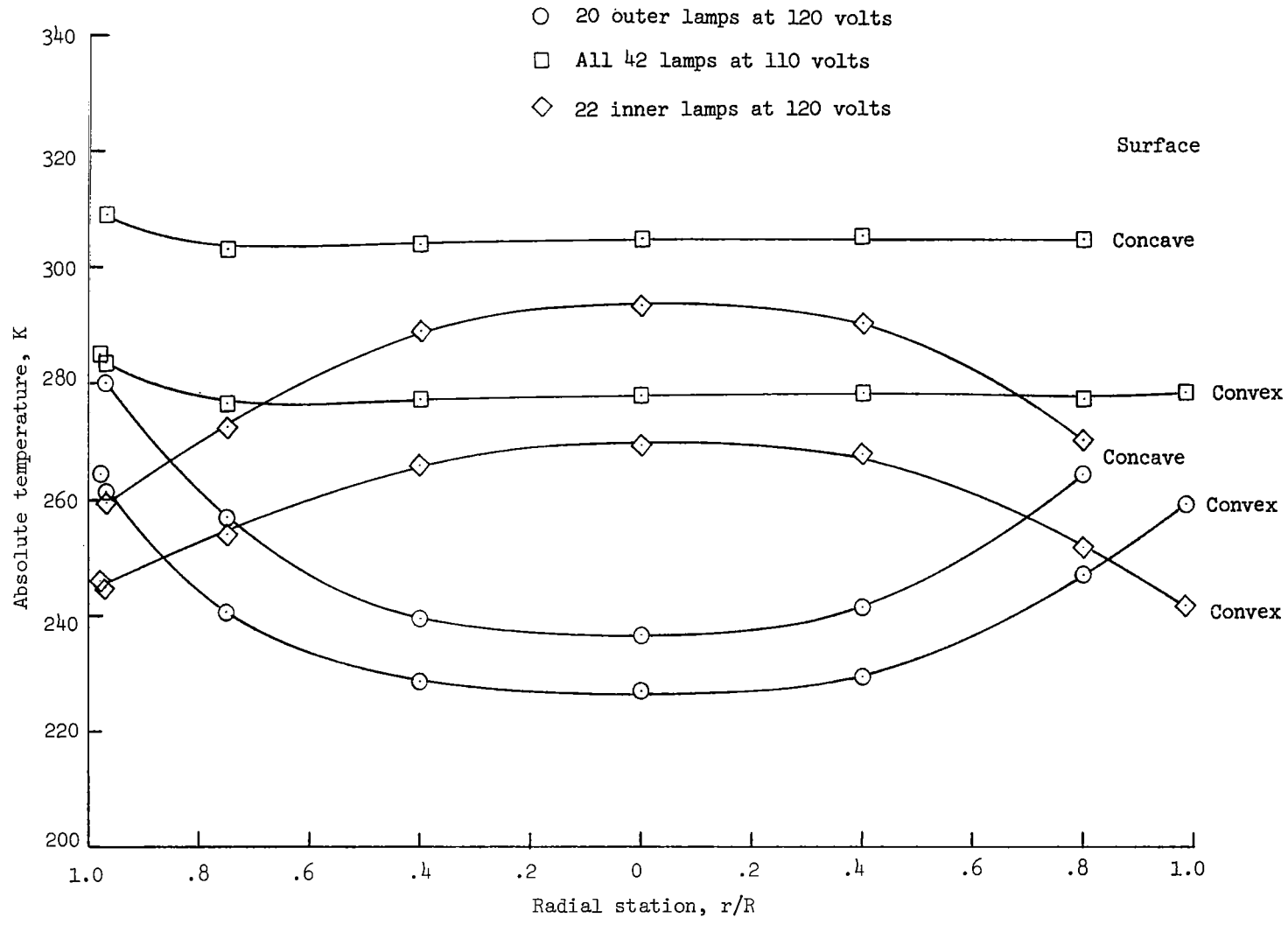

Figure 10.- Measured paraboloidal-shell surface temperatures along horizontal meridian for axisymmetrical irradiation. All 5 cryopanels cold.

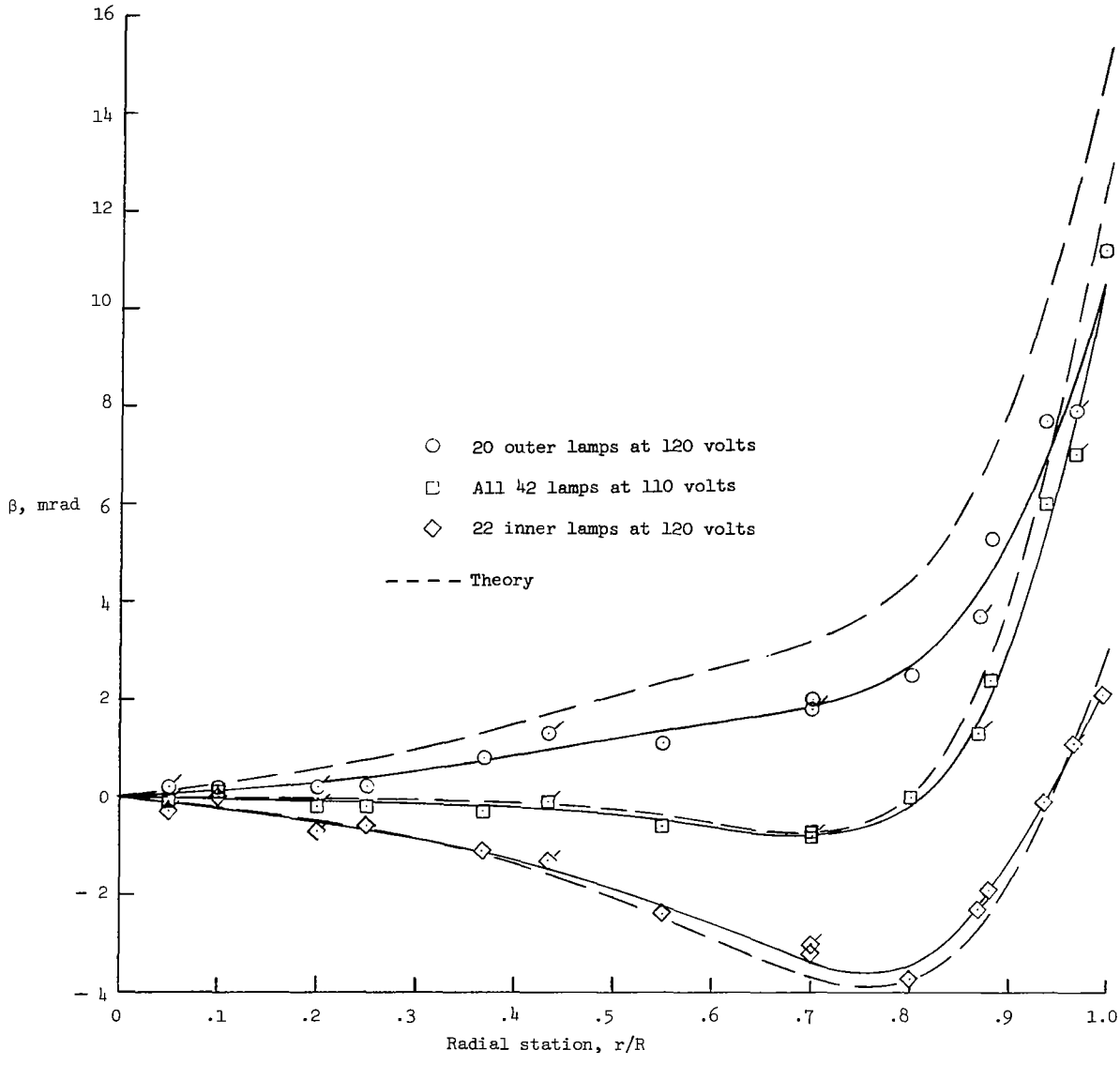

Figure 11.- Measured and theoretical rotation of paraboloidal-shell surface due to axisymmetrical temperature distributions. All 5 cryopanels cold. Flagged symbols represent right side of paraboloidal shell.

NASA-Langley, 1971 —— 32 L-7667